Journal of Biomedicine and Biosensors, 6(4):22–34, October-December: 2026.
DOI: https://doi.org/10.58613/jbb645

Journal of Biomedicine and Biosensors
ISSN (Online): 2583-3170

Journal homepage: https://www.gpub.org/journal-details.php?journal-id=45



Research Article

Low-Dose Radiation-Induced Epithelial-Mesenchymal Transition (EMT) and Paracrine Pro-Invasive Magnification in MCF-7 Cells

Raheem Abd Zaid AL-Abedi [1,2*], Khalidah Ibrahim Taifor [3], Ammar Hassan Mayah [2], Susan A. Brooks [2] and Munira Kadhim [2]

[1] *Department of Pathological Analysis, Faculty of Science, University of Kufa, Iraq.*
[2] *Department of Biomedical Science, Faculty of Health and Life Science, Oxford Brookes University, Oxford, UK.*
[3] *General Directorate of Education of Najaf Al-Ashraf, Najaf, Iraq.*
[*] *Corresponding author: raheema.alabedi@uokufa.edu.iq*

Article Info

Keywords: *Ionozing radiation, Low dose, EMT, N-cadherin, Beta-catanin, Invasion, Metastasis.*

Received: *10.09.2026;*
Accepted: *02.11.2026;*
Published: *06.11.2026*

© *2026 by the author's. The terms and conditions of the Creative Commons Attribution (CC BY) license apply to this open access article.*

Abstract

Background: Ionising radiation (IR) remains a cornerstone of breast cancer therapy, yet evidence indicates it can paradoxically promote malignant phenotypes in surviving cells. This study explored the contributions of direct irradiation versus exosome-mediated bystander signalling to epithelial-mesenchymal transition (EMT) and invasive potential in MCF-7 breast cancer cells under low dose of irradiation. **Methods:** MCF-7 cells were exposed to 0 Gy, 0.1 Gy, or 2 Gy X-ray irradiation, and invasion was quantified at early and late timepoints under direct irradiation and exosome-mediated bystander conditions. EMT markers (E-cadherin, Vimentin, N-cadherin, β-catenin) were assessed, and a Functional Invasion Efficiency Index (invasive cells per % N-cadherin) and Cadherin Switch Ratio (N-cadherin/β-catenin) were calculated. **Results:** Direct irradiation produced a non-linear response, peaking at 0.1 Gy ($\sim$1.74-fold invasion) and plateauing at 2 Gy ($\sim$4,800 cells/field). Exosome-mediated signalling drove progressive, dose-dependent escalation, reaching 11,385 cells/field at 2 Gy (late timepoint)—a 2.38-fold magnification over direct irradiation. The Functional Invasion Efficiency Index declined under direct irradiation (68.5 $\rightarrow$ 57.6) but surged with exosomes (70.3 $\rightarrow$ 129.7). Cadherin Switch Ratio increased dose-dependently (1.00 $\rightarrow$ 1.80 at 2 Gy), confirming EMT, though this was uncoupled from functional invasion under direct exposure. **Conclusion:** At clinically relevant radiation doses delayed sustained pro-invasive potentiation is the principal mechanism underlying bystander signalling and is mediated by exosomes which coordinate the upregulation of mesenchymal markers and invasion machinery. The results suggest that exosome-targeted approaches could be used in conjunction with radiotherapy, and also indicate the need for long-term monitoring after radiotherapy.

1. Introduction

Radiation-Induced Epithelial–Mesenchymal Transition in Breast Cancer

Although IR is an essential element in breast cancer treatment, recent evidence suggests that IR can paradoxically stimulate the expression of malignant phenotypes in cancer cells that survived the treatment, leading to treatment failure and disease progression. The epithe-

lial–mesenchymal transition (EMT) is a key mechanism by which irradiated cells become more migratory and invasive, and has now been recognized as a mechanism important for breast cancer radioresistance and metastasis [1]. Radiation Therapy is limited in its clinical efficacy because of the emergence of a subpopulation of tumour cells that have become radio-resistant, which can lead to tumour relapse and metastasis formation to other sites, thus emphasizing the importance of understanding the molecular mechanisms of radiation-induced phenotypic plasticity.

Radiation-induced EMT is characterised by coordination shift in cell adhesion molecule expression. Particularly, MCF-7 breast cancer cells, radiation has been shown to induce a substantial E-cadherin decrease and Vimentin–N-cadherin increase, with specific role of SLUG protein, which play an essential role, by sharply downregulating E-cadherin to support the mesenchymal phenotype [2, 3] . This reciprocal alteration—termed cadherin switching—represents a critical functional transition from epithelial cell–cell adhesion to a mesenchymal phenotype conducive to invasion and metastasis. Recent work has demonstrated that functional invasiveness and EMT are exacerbated together with altered glycosylation in MCF-7 cells irradiated with 2 Gy X-ray compared to control cells, with assessments conducted at 30 minutes, 4 hours, and 24 hours post-irradiation [4]. These findings indicate that despite the detrimental effects of 2 Gy X-ray IR on MCF-7 cells, a subpopulation of cells may have gained increased invasive potential, attributed to enhanced EMT and altered glycosylation, with deregulation of transforming growth factor-beta (TGF-β) following IR identified as a potential mediator lying at the intersection of these invasion-promoting cell processes. The role of TGF-β signalling in radiation-induced EMT has been further substantiated by studies demonstrating that TGFβ type I receptor signalling mediates histamine–ionising radiation crosstalk in EMT progression and cancer stem-like cell enrichment in breast cancer cells [4, 5].

1.1. Exosome-Mediated Bystander Effects and Pro-Invasive Signalling

Beyond the direct effects of radiation on exposed cells, non-irradiated cells within the tumour microenvironment can exhibit radiation responses through intercellular communication, collectively defined as radiation-induced bystander effects (RIBE). The core mechanism responsible for multidirectional communication of tumour cells and their associated microenvironment has emerged as exosome-mediated signalling which might result in enhancement of malignant tumour phenotypes [6]. AL-Abedi et al. (2021) conducted a pivotal investigation into exosome-mediated bystander effects of a 2 Gy X-ray therapeutic dose of ionising radiation on the invasive potential of MCF-7 breast cancer cells in vitro. Their findings demonstrated that exosomes derived from irradiated MCF-7 cells enhance invasiveness of bystander MCF-7 cells, possibly through altered miRNA and protein content carried in exosomes. This study provided direct evidence that extracellular vesicles serve as vehicles for the transfer of pro-invasive signals from irradiated to non-irradiated cells, establishing exosome-mediated paracrine signalling as a significant contributor to radiation-induced metastatic potentiation.

The molecular cargo of radiation-induced exosomes has been further characterized in subsequent studies. Radiation-induced exosomal miR-21 has been shown to enhance tumour proliferation and invasiveness in breast cancer, with high-dose irradiation-induced exosomes found to enhance tumour proliferation and invasiveness via the transfer of exosomal miR-21, contributing to poorer prognosis in breast cancer patients undergoing radiotherapy. Analysis of the TCGA database revealed that breast cancer patients with high levels of miR-21 have significantly reduced overall survival when treated with radiotherapy compared to those who did not receive radiotherapy, indicating a high hazard ratio for miR-21 in patients undergoing this treatment [7]. After 10 Gy irradiation, 4T1 cells secreted 2.20 ± 0.10 times more exosomes and exhibited a 1.85 ± 0.01-fold increase in exosomal miR-21 levels, and treatment with exosomes from 10 Gy-irradiated cancer cells led to enhanced tumour cell proliferation, wound healing, and migration. These findings suggest that radiation-induced exosomal miR-21 may contribute to a poorer prognosis of breast cancer patients undergoing radiotherapy.

Further evidence for the pro-invasive role of radiation-induced exosomes comes from studies examining their effects across multiple breast cancer cell lines [8]. Investigated the influence of ionising radiation on exosome properties and their ability to modify the sensitivity and biology of non-irradiated cells using exosomes isolated from MDA-MB-231, MCF7, and SKBR3 cell lines irradiated with 2 Gy or no irradiation. Despite some differences in their molecular profiles, exosomes did not affect cell viability, proliferation, cell cycle phase distribution, and radioresistance; however, both populations showed the ability to modify cell migration and invasion potential, as confirmed by the downregulation of β-catenin, which is responsible for maintaining the epithelial phenotype. Interestingly, exosomes from irradiated breast cancer cells were more actively deposited in endothelial cells, and exosomes tended to lower the expression of CD31, responsible for maintaining intact vascularity, demonstrating the vital role of exosomes and their altered profile due to irradiation in the pathobiology of breast cancer [8].

1.2. Low-Dose Hypersensitivity and Non-Linear Dose Responses

There is a significantly non-linear dose–response relationship between radiation and pro-invasive phenotypes, and a phenomenon of low-dose hyper-radiosensitivity (HRS) has been identified. The paradigm of low dose hyper-radiosensitivity and higher radioresistance (IRR) have been described in the breast cancer T-47D cells, with the cells below about 0.3 Gy apparently moving from G2 to mitosis without any attempt to repair the damaged DNA [9, 10].

These DNA Damaged, causing a significant loss of survival as a function of irradiation dose. This observation is in agreement with the idea that cells that have to undergo phenotypic plasticity might have greater sensitivity to low doses of radiation, which might have important therapeutic implications. The linker of nucleoskeleton and cytoskeleton complex has been shown to be required for X-ray-induced epithelial–mesenchymal transition, with studies demonstrating that low-dose (0.5 Gy or 2 Gy) X-irradiation induced EMT in human breast cancer MDA-MB-231 cells, further supporting the notion that low-dose radiation can trigger phenotypic transitions relevant to invasion and metastasis [4, 11].

The temporal dynamics of radiation-induced EMT have also been investigated with increasing precision. Time-course analyses have revealed that functional invasiveness and EMT are exacerbated together with altered glycosylation in MCF-7 cells irradiated with 2 Gy X-ray, with assessments at 30 minutes, 4 hours, and 24 hours post-irradiation capturing the evolution of these phenotypic changes. An increased rate of vimentin expression, one of the main markers of EMT, has been shown 48 hours after irradiation and at later time points tested in the study (up to 96 hours), indicating that radiation-induced EMT is a progressive phenomenon with delayed manifestations [4]. Time-course experiments have also shown that DLX2 protein levels were dramatically increased at 24 hours after irradiation in both A549 and MDA-MB-231 cell lines, with Smad2/3-regulated expression of DLX2 associated with radiation-induced EMT and radioresistance.

These temporal patterns underscore the importance of considering time-dependent effects when evaluating radiation-induced pro-invasive changes.

1.3. Cadherin Switching and Functional Invasion Efficiency

The dynamics of cadherin switching under ionising radiation exposure have been systematically evaluated through tracking the reciprocal expression levels of mesenchymal and epithelial markers. In MCF-7 cells, radiation-induced changes include a substantial E-cadherin decrease and Vimentin–N-cadherin increase, with the cadherin switch representing a functional transition from epithelial cell–cell adhesion to a mesenchymal phenotype. The E-cadherin and N-cadherin switch in epithelial-to-mesenchymal transition involves principal signalling pathways including TGF-β, Wnt/β-catenin, and Notch, and EMT increases cancer invasiveness and metastasis by upregulating mesenchymal markers including vimentin and N-cadherin, and downregulating epithelial markers such as E-cadherin [12, 13].

The functional relationship between mesenchymal marker expression and actual invasive output—which we term the "Functional Invasion Efficiency Index"—represents an underexplored dimension of radiation-induced EMT. While studies have documented changes in EMT markers following radiation, the quantitative relationship between N-cadherin expression and invasive capacity across varying radiation doses and exposure pathways has not been systematically characterized [12, 14–17]. In spite of that cadherin switch ratio is a functional indicator of epithelial–mesenchymal plasticity, (N-cadherin positivity/β-catenin positivity), the dose-dependent dynamics of this ratio when the cells are exposed directly versus via exosomes has not been completely understood. In addition to radiation, cadherin switching has been shown to be linked to therapy resistance in breast cancer; doxorubicin-resistant triple-negative breast cancer cells have increased expression of cyclin D1, β-catenin, N-cadherin, MMP-2, MMP-9, and ICAM-1 and decreased expression of CDH1 [18]. N-cadherin upregulation has also been shown to mediate adaptive radioresistance in glioblastoma, with cadherin junctions mediating β-catenin function and the N-cadherin C-terminus binding to β-catenin, α-catenin, and p120 catenin, further highlighting the functional significance of cadherin switching in radiation response [19].

1.4. Radiation-Induced Metastatic Potentiation and Tumour Microenvironment

The impact of radiation on metastatic potential extends beyond direct effects on cancer cells to encompass complex interactions with the tumour microenvironment. Local radiotherapy for murine breast cancer has been shown to increase risk of metastasis by promoting the recruitment of monocytic myeloid-derived suppressor cells (M-MDSCs) in the lung, with a series of in vitro experiments demonstrating how exosomes promote the recruitment of M-MDSCs in the lung of mice [20]. This finding highlights the systemic consequences of local radiation treatment and the role of exosomes as mediators of pro-metastatic signalling. Exosomes derived from radioresistant breast cancer cells have been shown to promote therapeutic resistance in naive recipient cells, with extracellular vesicles playing a role in the acquisition of radiotherapy resistance in triple-negative human breast cancer [8, 21]. Collectively, these observations suggest that radiation-induced exosomes contribute not only to enhanced invasiveness but also to the establishment of a pro-metastatic niche and acquisition of therapeutic resistance.

The clinical consequences of radiation-induced pro-invasive effects are considerable. Resent studies have shown that breast cancer patients with high levels of exosomal miR-21 have significantly reduced overall survival when treated with radiotherapy compared to those who did not receive radiotherapy, indicating that radiation-induced exosomal cargo may serve as a biomarker for poor prognosis and a potential therapeutic target [7]. Furthermore, co-treatment with vactosertib, a novel orally bioavailable activin receptor-like kinase 5 inhibitor, has been shown by others to suppress radiotherapy-induced epithelial-to-mesenchymal transition, cancer cell stemness, and lung metastasis of breast cancer, suggesting that targeting TGF-β signalling may mitigate radiation-induced pro-metastatic effects [2]. However, the relationship of mesenchymal marker and the associated parameters were not systematically quantified in these studies. Functional and non-functional invasive output in various radiation doses and pathways (direct vs exosome mediated).

The present study addresses this gap by developing quantitative metrics—the Functional Invasion Efficiency Index and Cadherin Switch Ratio—to assess radiation-induced epithelial-mesenchymal plasticity in MCF-7 cells, thereby providing a framework that may inform future therapeutic strategies targeting exosome-mediated pro-metastatic signalling.

2. Materials and methods

2.1. Cell Culture

MCF-7 human breast cancer cells were maintained in Dulbecco's Modified Eagle's Medium (DMEM) supplemented with 10% fetal bovine serum (FBS), 1% penicillin-streptomycin, and 2 mM L-glutamine at 37°C in a humidified atmosphere of 5% CO. Cells were routinely subcultured upon reaching 70–80% confluence and used within 20 passages. Cell viability was confirmed to exceed 95% prior to all experiments using trypan blue exclusion.

2.2. Irradiation Procedure

X-ray source (the MXR321 X-ray machine at 250 kV constant potential, 14 mA) has been used to irradiate cells at room temperature with dose rate of approximately 0.5 Gy/min . Three dose conditions were employed throughout: 0 Gy (sham-irradiated control), 0.1 Gy (low dose), and 2 Gy (clinically relevant high dose). Non-irradiated controls were handled identically but shielded from radiation. Dosimetry was verified prior to each experiment.

2.3. Exosome Isolation and Characterization

Conditioned media of the irradiated (0, 0.1, 0.5, or 2 Gy) and control MCF-7 cells were used to isolate exosomes by differential centrifugation at 300 × g for 10 min, 2,000 × g for 20 min, 10,000 × g g for 30 min and subsequent ultracentrifugation at 100,000 × g g for 70 min at 4°C,

followed by washing with PBS and re-centrifugation. The exosome concentration and size distribution were determined by nanoparticle tracking analysis (NTA) and transmission electron microscopy (TEM). The exosomes (10 µg/mL) were added to the bystander cells throughout the assay.

2.4. Invasion Assay

Cellular invasion was assessed using Matrigel-coated Transwell inserts (8 µm pore size). MCF-7 cells (5×10^4 per insert) were seeded in serum-free medium in the upper chamber, with 10% FBS-containing medium as chemoattractant in the lower chamber. Two exposure routes were compared: (i) direct irradiation, where cells were irradiated prior to seeding; and (ii) exosome-mediated bystander exposure, where non-irradiated cells were treated with exosomes harvested from irradiated or control cells. Invasion was quantified at two timepoints: early (24 h) and late (48 h post-exposure). Non-invading cells were removed, and invaded cells were fixed, stained with crystal violet, and counted in five randomly selected optical fields per insert under light microscopy ($\times$ 200). Results are expressed as invasive cells per field.

2.5. Immunocytochemistry for EMT Biomarkers

N-cadherin, Vimentin, E-cadherin and β-catenin expression was assessed by immunocytochemistry. Cells were cultured on chamber slides, fixed in 4% paraformaldehyde, permeabilized with 0.1% Triton X-100, and blocked with bovine serum albumin. Cells were incubated overnight at 4°C with primary antibodies against E-cadherin, Vimentin, N-cadherin, or β-catenin, followed by incubation with appropriate fluorophore-conjugated or HRP-conjugated secondary antibodies. Negative controls were processed identically with omission of primary antibody. Stained cells were visualized by light or fluorescent microscope, with biomarker positivity being defined as the presence of a positive test in either, or both, of these microscopes. Quantified using the number of cells that stained positively in five randomly selected fields per condition, given as percentage of all cells counted.

2.6. Derived Metrics and Data Transformation

Three derived metrics were calculated from the primary invasion and biomarker data:

Fold increase in invasion: invasive cell count at each dose ÷ invasive cell count at 0 Gy baseline (set to 1.0), calculated separately for direct irradiation and exosome exposure. Functional Invasion Efficiency Index: invasive cells per field ÷ percentage of N-cadherin positivity, calculated for each dose and exposure route. Cadherin Switch Ratio: N-cadherin positivity (%) ÷ β-catenin positivity (%), calculated for each dose. Exosomal Bystander Pro-Invasive Magnification Factor: invasive cells under exosome exposure ÷ invasive cells under direct irradiation at the same dose and timepoint, with an equivalence baseline of 1.0.

2.7. 3D Response Surface Mapping

To create a visual representation of the combinatory effect of radiation dose and exposure timepoint on invasive capacity, a three-dimensional response surface was built based on the variables: Radiation Dose (x-axis: 0-2 Gy), Timepoint (y-axis: 1.0 = early, 2.0 = late) and Invasive Cell Count per Field (z-axis). The dosetime matrix for the exosome mediated condition was interpolated to create a surface topology, with color gradients representing the level of invasion for the cells.

2.8. Statistical Analysis

All experiments were performed in triplicate (n = 3 independent biological replicates), with data presented as mean ± standard deviation (SD). Comparisons between direct irradiation and exosome-mediated conditions across doses (0, 0.1, 2 Gy) and timepoints (early, late) were performed using two-way analysis of variance (ANOVA) followed by Tukey's post hoc test for multiple comparisons. Dose-response relationships within each exposure route were assessed by one-way ANOVA with Dunnett's post hoc test against the 0 Gy control. The non-linear low-dose hyper-sensitivity profile Figure 4A was evaluated by comparing fold-change values across doses using the Kruskal-Wallis test where normality assumptions were not met, with Dunn's post hoc correction. Biomarker positivity comparisons across doses Figures 4B and Figure 5 were analyzed by one-way ANOVA with Tukey's post hoc test. Magnification ratios Figure 3 were compared against the equivalence baseline (1.0) using one-sample t-tests. A p-value < 0.05 was considered statistically significant. All analyses were conducted using GraphPad Prism (version 9.0) or equivalent statistical software.

3. Results

3.1. Time-Dependent Potentiation of Invasive Potential in MCF-7 Cells

The data showed a significant enhance in the invasive capacity of MCF-7 in both dose of irritation and dose dependent manner demonstrates that both direct radiation exposure and exosome-mediated paracrine signalling. At starting point (0 Gy control), direct irradiation demonstrated an increase in the invasive cell count of approximately 3,250 cells/field across both early and late timepoints, meanwhile, the exosome-mediated bystander effect shows an elevation in basal invasion levels (∼4,800 to 4,910 cells/field). Moreover, exposure to low-dose radiation (0.1 Gy), direct irradiation induces a noticeable increase in invasion to around 5,700 cells/field, which remains static between the early and late timepoints. In contrast, the bystander effect of exosome at 0.1 Gy demonstrates a sharp early invasion response (∼6,900 cells/field) that slightly contracts to 6,482 cells/field at the late timepoint. Furthermore, The most outstanding increase in the number of invasion cells were occurs at a higher radiation dose (2 Gy): while direct irradiation plateaus at around 4,800 cells/field, the exosome effect exhibits a marked temporal surge, escalating from ∼6,600 cells/field at the early timepoint to a peak of 11,385 cells/field at the late timepoint. These findings highlight that exosome-mediated bystander factors exert a stronger, time-dependent pro-invasive magnification compared to direct irradiation alone, particularly at higher radiation doses Figure 1.

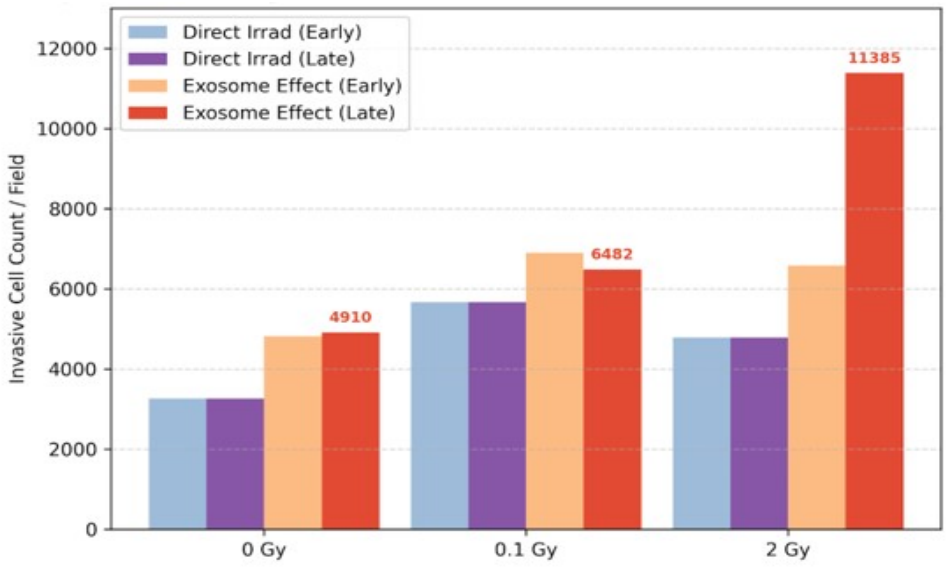


Figure 1: Time-Dependent Potentiation of Invasive Potential in MCF-7 Cells Under Direct Radiation and Exosome-Mediated Paracrine Signalling. Direct irradiation increases invasion to a modest plateau (∼5,700 cells/field at 0.1 Gy and ∼4,800 cells/field at 2 Gy), the exosome-mediated bystander effect exhibits marked pro-invasive magnification, peaking at 11,385 invasive cells/field at the late timepoint under 2 Gy conditions. Values represent invasive cell counts per optical field

3.2. Functional Invasion Efficiency Index: Invasive Capacity / Mesenchymal Marker

The relationship between cellular invasive yield and N-cadherin expression across direct irradiation and exosome-mediated conditions at varying radiation doses. In the experimental control conditions (0 Gy), both direct irradiation and exosome exposure display similar efficiency values, yielding 68.5 and 70.3 invasive cells per percentage of N-cadherin expressed, respectively. At 0.1 Gy, a low radiation dose, direct irradiation slightly decreases the invasion yield to 66.0. Meanwhile, the exosome-mediated effect increases efficiency to 80.1. The disparity becomes pronounced at 2 Gy: direct irradiation drops further to an index value of 57.6, while the exosome effect undergoes a dramatic surge, reaching a peak efficiency index of 129.7. This marked divergence demonstrates that while direct irradiation leads to a diminishing functional invasion yield per unit of N-cadherin at higher doses, exosome-mediated paracrine signalling significantly magnifies the functional invasive output relative to mesenchymal marker expression as shown in Figure 2.

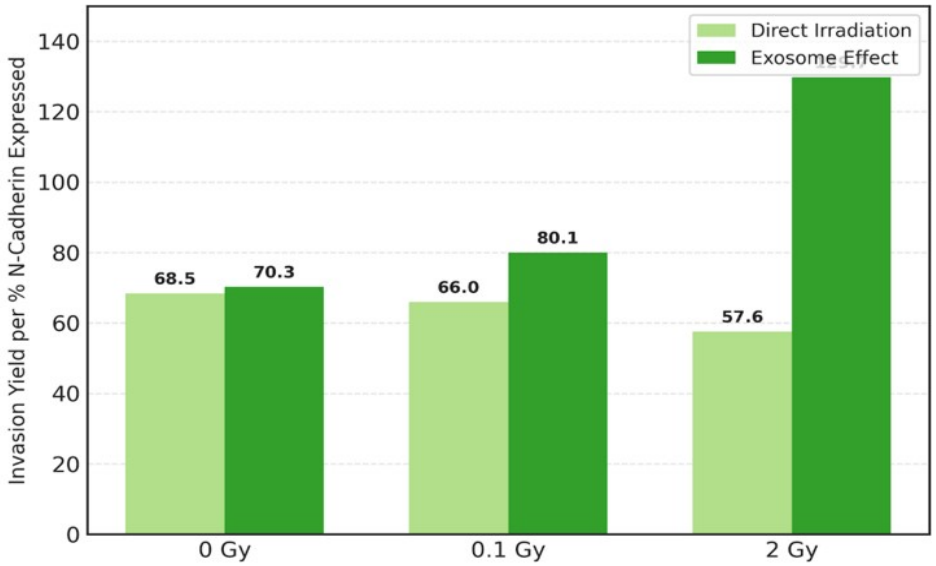


Figure 2: Functional Invasion Efficiency Index Across Radiation Doses and Exposure Pathways. Quantification of cellular invasion yield normalized per percentage of N-cadherin expression (Invasive Capacity / Mesenchymal Marker) in MCF-7 cells under direct irradiation versus exosome-mediated paracrine signalling. At baseline (0 Gy) and low dose (0.1 Gy), invasion efficiency remains comparable between conditions, ranging from 57.6 to 80.1 invasive cells per % N-cadherin expressed. At 2 Gy, direct irradiation results in a reduced functional yield (57.6), whereas exosome-mediated signalling exhibits a pronounced surge to an index value of 129.7, demonstrating enhanced functional invasive efficacy relative to mesenchymal biomarker levels

3.3. Exosomal Bystander Pro-Invasive Magnification Factor

The data represents the fold change in cellular invasion caused by exosome exposure relative to direct irradiation (Exosome / Direct) with an equivalence baseline of 1.0. The paracrine magnification ratio is always greater than 1.0 for all radiation doses and time points, suggesting that the pro-invasive response is stronger via exosome-mediated pathways than direct exposure. The invasion is increased by 1.48 folds at the early time point in comparison to the direct control at baseline (0Gy) and 1.51 folds at the late time point in comparison to the direct control at baseline (0Gy). This relative gain is slightly reduced under low dose radiation, to 1.22x at early stage and 1.14x at late stage, still exceeding the equivalence limit. The biggest increase is seen at 2 Gy: at the early timepoint, the increase is 1.37 fold, whilst at the late timepoint there is a significant increase of 2.38 fold. These findings reveal a potent dose- and time-dependent magnification effect, with exosomes obtained from the higher doses resulting in a delayed, but significant increase in invasion potential as demonstrated in the results shown above Figure 3.

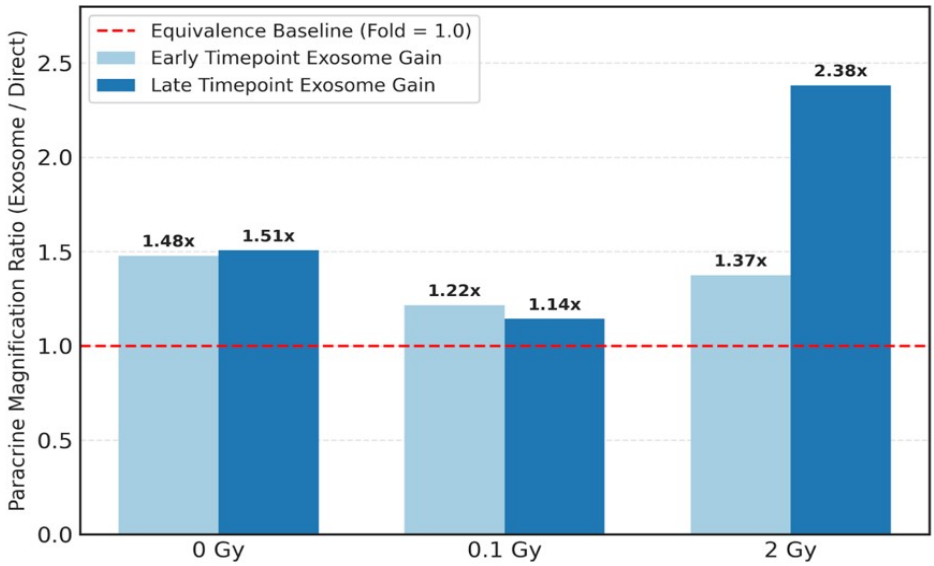


Figure 3: Exosomal Bystander Pro-Invasive Magnification Factor Across Radiation Doses and Timepoints. The paracrine magnification ratio (invasive cell) was quantified. The escape rate of each escape-under-exposure population, relative to escaping under direct irradiation (Exosome/Direct), was calculated within each population. Three different conditions: 0 Gy (control), 0.1 Gy (low-dose), and 2 Gy (radiation). The dashed red line, the equivalence baseline (fold change = 1.0) is denoted by. All conditions are greater than baseline. The baseline (0 Gy) group showed 1.48x (early) and 1.51x (late) increases, and low-dose (0.1) 1.45x (early) and 1.52x (late) increases were observed. The increases for Gy are 1.22x (early) and 1.14x (late). Exosomes are exposed to 2 Gy irradiation. Exp. of exosomes to 2 Gy radiation. shows significant time-dependence amplification (to 1.37x at a shift towards an increased ratio of 2.38x at the late timepoint, indicative of improved bystander invasion over time after higher dose irradiation

3.4. Non-Linear Low-Dose Hyper-Sensitivity and Biomarker Dynamics in Irradiated MCF-7 Cells

The data demonstrate the dose-dependent behavioural and biomarker shifts induced by direct radiation and exosome-mediated signalling across 0 Gy, 0.1 Gy, and 2 Gy treatments as shown in Figure 4.

3.4.1. Panel A: Non-Linear Pro-Invasive Response

The fold increase in invasion compared to an un-irradiated control (0 Gy baseline = 1.0) is analyzed in Panel A. A non-linear, hyper-sensitivity profile is apparent with direct irradiation and a high fold increase around 0.1 Gy for cellular invasion of $\sim$1.74. When the radiation dose is raised to 2 Gy, however, there is a paradoxical reduction with direct invasion decreasing to $\sim$1.47-fold above basal. In contrast, the dose-dependent response is upward with the exosome-mediated response. Exosome treatment is found to have a moderate effect on invasion at 0.1 Gy (1.32-fold) with a dramatic acceleration at 2 Gy ($\sim$2.32-fold). This highlights a mechanistic divergence, where direct radiation inductions low-dose hyper-sensitivity while exosome-mediated bystander effects scale progressively with higher radiation doses.

3.4.2. Panel B: Low-Dose (0.1 Gy) Hyper-Sensitivity

To follow the corresponding phenotypic transition, the key epithelial-mesenchymal transition (EMT) markers are reported by PeakPanel B. Epithelial marker E-cadherin is highly expressed (90%) and mesenchymal marker Vimentin is less expressed (47.5%) in the untreated control (0 Gy). A sharp biomarker inversion is observed after low dose exposure (0.1 Gy), corresponding to the hyper-sensitivity peak: Vimentin positivity rises to 87.2% and E-cadherin expression is at its lowest level (56.7%). The phenotypic change is partially reversed at 2 Gy, with Vimentin slightly reduced to 84.2% and E-cadherin slightly increased to 65.8%. The reciprocal expression of E-cadherin suppression and Vimentin gain when compared with control underscores the ability of low doses of radiation (0.1 Gy) to induce a rapid EMT phenotype switch in MCF-7 cells.

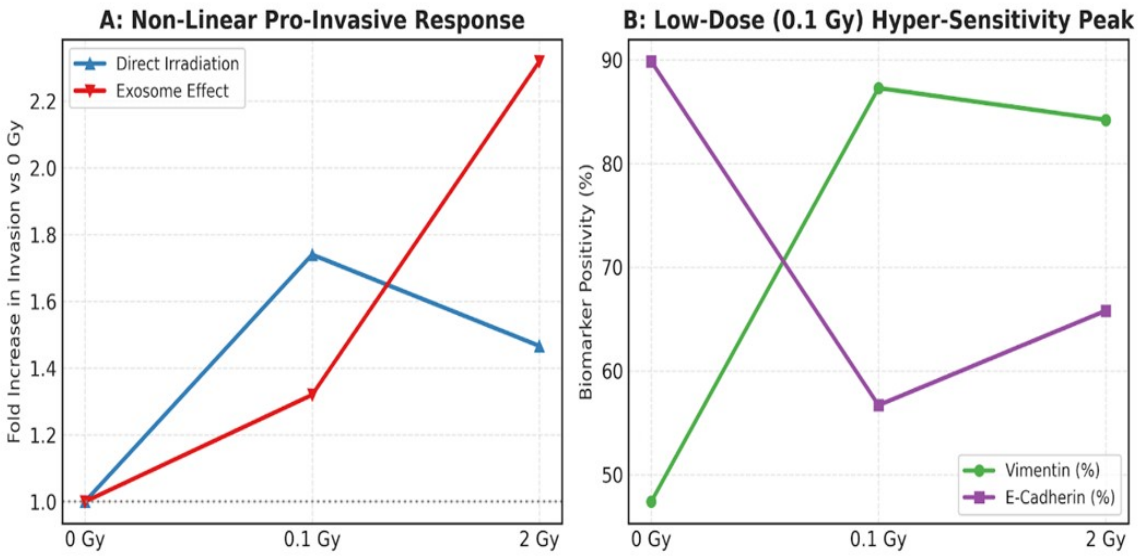


Figure 4: Non-Linear Low-Dose Hyper-Sensitivity and Biomarker Inversion in Irradiated MCF-7 Cells. (A) at 0.1 Gy, the relative invasion fold increase compared to baseline (0 Gy = 1.0), displaying a low-dose hyper-sensitivity peak (∼1.74-fold), under direct irradiation versus a dose-dependent escalation under exosome exposure increases by (∼2.32-fold at 2 Gy). (B) EMT biomarker dynamics showing a reciprocal inversion at 0.1 Gy, categorised by a sharp loss of epithelial E-cadherin (90% to 56.7%) and a concomitant surge in mesenchymal Vimentin positivity (47.5% to 87.2%)

3.5. Dose-Dependent Shift in β-Catenin and N-Cadherin Expression

The dynamics of cadherin switching under ionising radiation exposure were evaluated by tracking the reciprocal expression levels of the mesenchymal marker N-cadherin and the cell junctional protein Beta-catenin across 0 Gy, 0.1 Gy, and 2 Gy radiation conditions. In baseline control cells (0 Gy), expression of Beta-catenin (71.5%) and N-cadherin (70.1%) remained in near-equimolar parity, yielding a baseline Cadherin Switch Ratio (N-cadherin / Beta-catenin) of 1.00. After low-dose exposure (0.1 Gy), cells underwent the initial EMT transition with a moderate decrease in the expression of Beta-catenin to 63.8%, and the concurrent increase in the expression of N-cadherin. This expression rose to 81.0%, and the Cadherin Switch Ratio increased to 1.27.

The reciprocal deviation became deeply obvious at a higher radiation dose (2 Gy). Beta-catenin positivity underwent a sharp reduction down to 48.7%, reflecting a significant loss of epithelial cell-cell adhesion integrity. Concurrently, N-cadherin expression escalated to a peak of 87.8%, denoting substantial mesenchymal phenotype acquisition.

In the overall Cadherin Switch Ratio experienced, reaching a maximum ratio of 1.80 at 2 Gy, with 80% increase relative to baseline. These quantitative shifts demonstrate a clear dose-dependent transition from epithelial cell-cell adhesion to a mesenchymal phenotype driven by loss of junctional Beta-catenin and gain of N-cadherin.

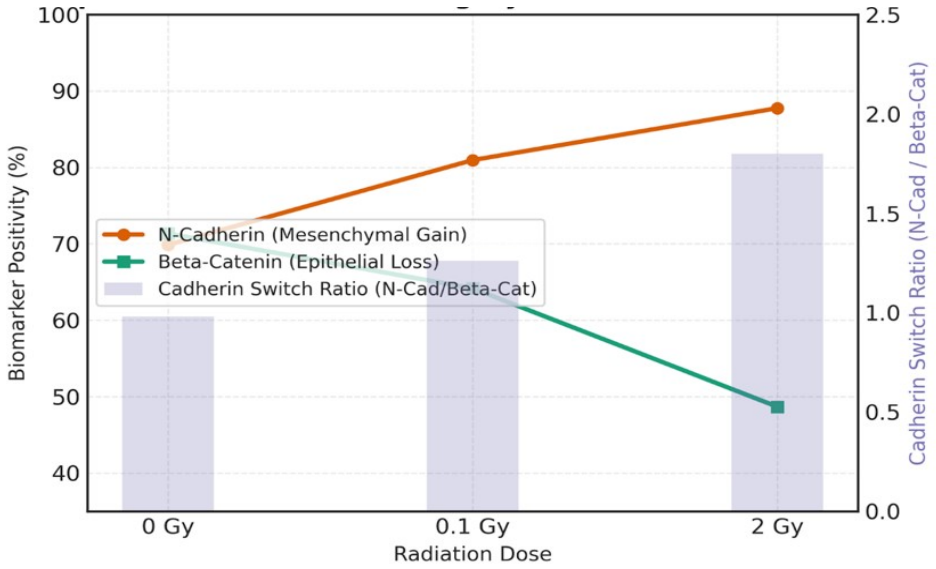


Figure 5: Reciprocal Cadherin Switching Dynamics and Cadherin Switch Ratio Across Radiation Doses. Adhesion to a mesenchymal phenotype in MCF-7 cells after exposure to 0 Gy quantitative assessment of the transition from epithelial cell-cell. After low-dose (0.1 Gy) and control (0 Gy) exposure, the number of cells that were found to be in adhesion to the mesenchymal phenotype was higher in the low-dose group than in the control group in MCF-7 cells, and 2 Gy radiation conditions. Biomarker positivity percentages (orange line with circles; mesenchymal gain and green line with squares; epithelial loss) are plotted on the left axis

Right y-axis represents the functional Cadherin Switch Ratio (purple bars; N-cadherin positivity /) beta-catenin positivity Ionising radiation not only caused a dose-dependent decrease in junctional beta-catenin (from 71.5% to 48.7%) but also led to a corresponding increase in expression of N-cadherin (from 70.1% to 87.8%).

The Cadherin Switch Ratio increases from 1.00 at 0 Gy to a peak value of 1.80 at 2 Gy, revealing significant epithelialmesenchymal plasticity induced by radiation.

3.6. Time-Dependent Potentiation of Invasive Potential Under Direct Irradiation vs. Exosomal Bystander Signalling

To evaluate the differential contribution of direct cellular irradiation and exosome-mediated paracrine signalling to tumor aggressiveness, MCF-7 cellular invasion was quantified across three radiation regimens (0 Gy control, 0.1 Gy low dose, and 2 Gy high dose) at both early and late post-exposure timepoints. Under baseline non-irradiated conditions (0 Gy), direct exposure yields a static invasive cell count of approximately 3,250 cells/field across both early and late observation windows. Treatment with control-derived exosomes induces a baseline pro-invasive enhancement, elevating invasion counts to 4,800 cells/field at the early timepoint and peaking at 4,910 cells/field at the late timepoint Exposure to low dose ionising radiation (0.1 Gy) generates different responses along pathways: Direct Irradiation: Evokes a significant increase of ∼75% over the non-irradiated controls, with a level of ∼5,700 (early and late). Exosomal Signalling: Continued to induce an additional increase in invasion, reaching the early time point of ∼6,900 cells/field and then stabilizing at 6,482 cells/field at the late time point. Exposures through the direct route: At a therapeutic clinical dose (2 Gy) it is observed that there is a relative plateau or contraction compared to the low dose exposure, and that there is no significant change at early or late time points (>∼4,800 invasive cells/field). Exosomal Signalling: Demonstrates a strong temporal escalation. The early timepoint shows ∼6,600 cells/field (close to the level of low-dose exosome timepoint), whereas a dramatic ∼1.72-fold increase compared to its early timepoint counterpart is seen at the late timepoint with up to 11,385 invasive cells/field. These quantitative findings demonstrate that while direct physical irradiation induces a low-dose saturation in cell invasion, exosome-mediated bystander signalling triggers a potent, dose- and time-dependent magnification of invasive capacity. This suggests that extracellular vesicle-mediated paracrine factors serve as a primary vehicle for delayed, radiation-induced metastatic potentiation as shown in Figure 6.

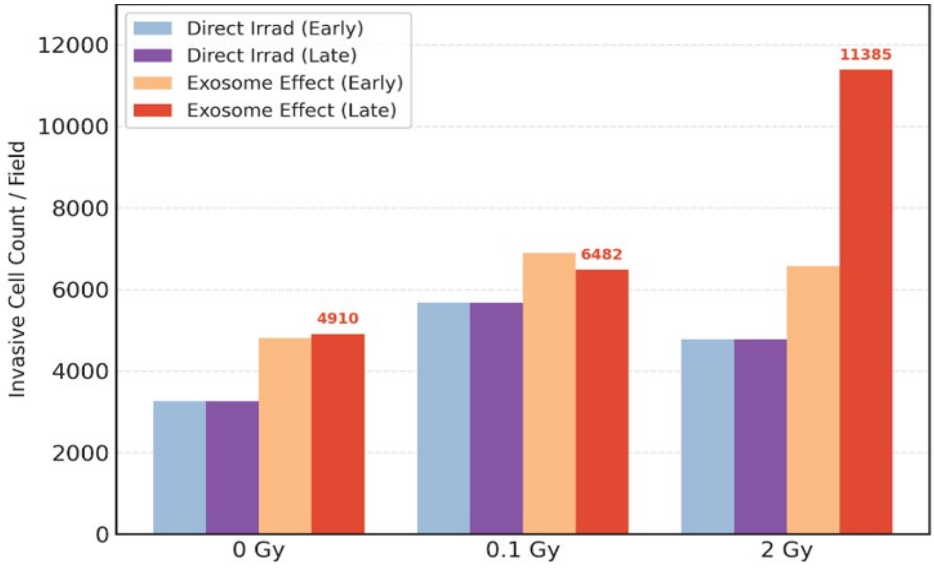


Figure 6: Time-Dependent Potentiation of Invasive Potential in MCF-7 Cells Under Direct Radiation and Exosome-Mediated Paracrine Signalling. Measurement of invasive cell number per optical field in MCF-7 cells after direct irradiation (light/dark purple) and after irradiation by harvested exosomes (light/dark orange-red) at early and late times following 0 Gy, 0.1 Gy and 2 Gy radiation doses. The non-linear saturation response for direct irradiation is observed with a peak value of ∼5,700 cells/field at 0.1 Gy and plateau value of ∼4,800 cells/field at 2 Gy. In contrast, bystander signalling by exosomes is a dramatic magnification of the invasive potential, from 4,910 cells/field at 0 Gy late to 11,385 cells/field at 2 Gy late. Values represent the mean of cell counts that were invasively counted in a field

3.7. The response surface topology shows a clear non-linear, multi-phasic relationship between dose escalating factors and time progression

At the baseline and early dynamics (Timepoint 1.0), the invassive cells show a moderate baseline at 0 Gy around 4900-5000 cells/field, and that were an increase to to intermediate plateau (cell invasion ∼6600-6900 cells/field) from low to high radiation doses (0.1 Gy to 2.0 Gy). The temporal trajectory of cell loss is relatively flat (6,900 to 6,482 cells/field) at low doses (0.1 Gy), suggesting early effects (1.0) do not lead to a subsequent flow (2.0). At high radiation dosage (2.0 Gy), the response surface shows a steep, synergistic trend towards the late timepoint (2.0). Maximum peak of the surface is greater than 11,300 cells/field (dark red region). This 3D landscape shows that there is a shift towards pro-invasion at early time points after low doses of radiation, which evolves into a strong time-dependent compounding effect after therapeutic radiation doses (2.0 Gy) and reveals a strong pro-invasive surge at later time points.

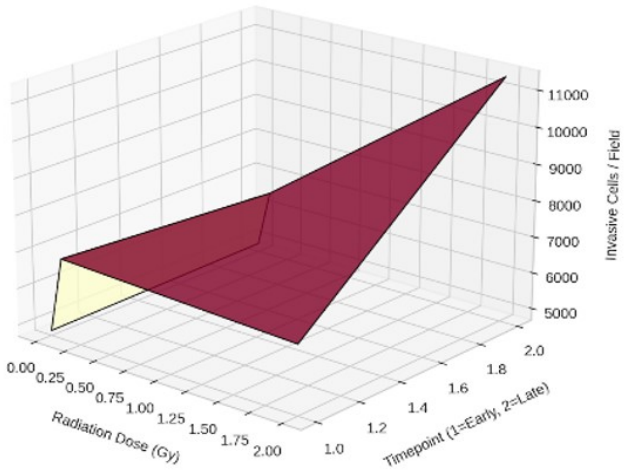


Figure 7: The 3D Response Surface Mapping Radiation Dose vs. Timepoint vs. Invasion is a non-linear design.3D Response Surface Mapping Radiation Dose vs. Timepoint vs. Invasion is a non-linear design. The interactive dynamics of the three variables (three-dimensional surface topology), relating to Radiation Dose (0 to 2 Gy), Exposure Timepoint (1.0 = Early, 2.0 = Late), and cellular invasiveness (Invasive Cells / Field) are illustrated. At early timepoints, cell invasion is on a level plateau (∼5,000–6,900 cells/field), before reaching a maximum invasion at the late timepoint under 2 Gy exposure (>11,300 cells/field). Color transitions represent the relative density of invasive cell counts and reflect a progressive, dose-dependent increase in invasive potential that occurs with a time delay

4. Discussion

4.1. Time-Dependent Potentiation of Invasive Potential: Direct Irradiation versus Exosomal Bystander Signalling

The data shown in Figure 1 suggest that there is a very fundamental difference between the trajectories of invasion induced by direct irradiation and the ones that are induced by bystander signalling through exosomes. The direct irradiation produced a small saturating response with an increase in the number of invading cells reaching a peak at ∼5,700 cells per field at 0.1 Gy, followed by a decrease to ∼4,800 cells/field at 2 Gy, with no change at early and late timepoints. In contrast, exosomes isolated from irradiated MCF-7 cells produced a gradual and dose-dependent escalation, reaching 11,385 invasive cells/field at the late timepoint after 2 Gy of radiation—an almost 2.4-fold increase over the number of direct-irradiated cells under the same conditions Figure 3.

This is similar to the basic concept of Al-Abedi et al. that irradiated exosomes from MCF-7 cells increase the invasiveness of bystander cells by changing their miRNAs and protein cargo [4]. The results here indicate that the exosomal effect is not just additive, but cumulative: DNA damage can promote pro-invasive signalling to a maximum, presumably due to the trade-offs between DNA damage, apoptosis and senescence, while exosome-mediated paracrine signalling acts as a prolonged and delayed amplifier. The early exosomal effect at 2 Gy (∼6,600 cells/field) was similar to the low dose levels, but the late effect at >11,000 cells/field suggested a need for time for the molecular cargo carried by the exosomes to be able to reprogram the recipient cells to a fully invasive phenotype. This temporal dissociation is consistent with the known exosome uptake, processing of cargo, and subsequent transcriptional remodelling, and indicates that the therapeutic window to reverse radiation-induced metastatic potentiation could possibly be quite prolonged.

This observation of an increase in basal invasion from control-derived exosomes (0 Gy) at ∼4,800–4,910 cells/field compared to the basal invasion of direct 0 Gy controls at ∼3,250 cells/field should be considered. This basal exosomal effect may be due to the natural content of the exosomes of the MCF-7 cell, which could contain pro-migratory factors that are not affected by radiation. This radioconstitutive background is thus added to the radiation-dependent increment, which is a true radiation-specific potentiation and not a nonspecific exosomal effect.

4.2. Functional Invasion Efficiency Index: Decoupling Mesenchymal Marker Expression from Invasive Output

Measurements that we introduce in this work, the invasion yield per percentage of N-cadherin expression, reveals a critical dissociation between expression of the biomarker and functional behavior, as illustrated in Figure 2. In direct irradiation, this efficiency index decreased with doses (68.5, 66.0, 57.6): In direct irradiation, the expression of N-cadherin increased Figure 5 with a reduction in the actual output of invasion per unit of mesenchymal marker. The pattern observed suggests that the upregulation of N-cadherin by direct radiation might be a stress response that is not tightly linked to functioning invasion machinery or that radiation-induced damage of cytoskeletal and matrix-degrading machinery limits the ability of the mesenchymal phenotype to become invasive.

Unlike in the direct irradiation cells, the efficiency index of the exosome-exposed cells gradually increased up to 129.7 at 2 Gy, which is over 2 times higher than the value obtained with direct irradiation at the same dose. The divergence suggests that exosomal cargo is not simply involved in the induction of N-cadherin expression, but also in the co-regulation of downstream cellular effectors that are needed to mediate the adhesion switch into functional invasion. Mediators that have been described as potential targets for exosomal miR-21 include members of the matrix metalloproteinase (MMP) family, cytoskeletal regulators, and metabolic enzymes, which are all properties that could promote proliferation, wound healing, and migration in breast cancer models [4, 5]. The Functional Invasion Efficiency Index is therefore a

conceptually useful way to differentiate functionally important changes to the phenotypes from changes that may be epiphenomenal, and which can have direct implications for the development of biomarkers.

4.3. Exosomal Bystander Pro-Invasive Magnification: Dose- and Time-Dependent Amplification

As seen in Figure 3, all the paracrine magnification ratios are greater than the direct irradiation, and the effect is not linear, being greater the lower the amount of direct irradiation. The ∼1.5-fold exosomal gain at 0 Gy is most likely due to the presence of exosomal cargo that is always present. The ratio became smaller at 0.1 Gy, 1.22 (early) and 1.14 (late), indicating that the effect of the direct irradiation alone is already sufficient at that dose level to close the gap between direct and paracrine effects. The most striking result here is the 2 Gy late-timepoint ratio of 2.38, indicating that high dose irradiation of cells fundamentally changes exosomal content, resulting in long-term, but deep, pro-invasive amplification.

This dose-dependence is not unprecedented; exosomes from irradiated breast cancer cells were shown to regulate the migration and invasion potential of multiple cell lines in a dose-dependent manner, with a reduction in β-catenin suggested to be responsible for the loss of epithelial integrity [22]. The present data further quantify the timeliness of the effect and show that there is a qualitative improvement in the potency of exosomes when the amount of two Gy is exceeded. Clinically, this is the typical fraction size used in traditional radiotherapy, suggesting that the dose used to achieve local control may result in the simultaneous induction of signals that promote dissemination in distant organs which would need to be validated in in vivo models but may have implications for fractionation schedules and/or adjuvant therapies targeting exosomal dissemination.

4.4. Non-Linear Low-Dose Hyper-Sensitivity and the Biomarker Inversion at 0.1 Gy

The dose response for invasion under direct irradiation appears to be non-linear, with the fold increase reaching a maximum of ∼1.74-fold at 0.1 Gy, and then decreasing at 2 Gy (fold increase of ∼1.47-fold) Figure 4A; the dose response for the exosomes was monotonic, with a fold increase of ∼2.32-fold at 2 Gy Figure 4B.This pattern is consistent with the phenomenon of low-dose hyper-radiosensitivity (HRS), in which cells below approximately 0.3 Gy proceed from G2 to mitosis without repairing DNA damage, leading to disproportionate biological effects [8, 23, 24]. The present data suggest that this low-dose window may be particularly permissive for acute phenotypic transitions, a concern relevant to fractionated radiotherapy in which small daily doses are delivered.

The biomarker dynamics in Figure 4B provide mechanistic insight into this low-dose window: at 0.1 Gy, Vimentin positivity in low doses (0.1 Gy) shows a significant increase (87.2%) along with a corresponding decrease in E-cadherin to 56.7% which shows maximum mesenchymal shift among the low doses tested Figure 4B. This EMT response was only partially recovered at 2 Gy (Vimentin 84.2%, E-cadherin 65.8%), indicating that at larger doses, the acute EMT signal can be counterbalanced by other stresses induced by radiation. This is confirmed by the reported ability of radiation to cause senescence and apoptosis in a dose-dependent fashion, decreasing the number of cells that can express a 'mesenchymal' phenotype. Importantly, the exosomal pathway avoids these direct cytotoxic effects on the recipient cell, which allow progressive phenotypic reprogramming in the absence of confounding direct DNA damage, as is the case with each of the other exposure routes [25].

4.5. Reciprocal Cadherin Switching and the Cadherin Switch Ratio

Figure 5 documents a dose-dependent cadherin switch: β-catenin declined from 71.5% (0 Gy) to 63.8% (0.1 Gy) to 48.7% (2 Gy), while N-cadherin rose from 70.1% to 81.0% to 87.8%, yielding Cadherin Switch Ratios of 1.00, 1.27, and 1.80, respectively. The ratio increased by 80% at 2 Gy, signifying a significant change from an epithelial to a mesenchymal cell phenotype.

The results are consistent with the well-known paradigm of cadherin switching during EMT, in which the loss of E-cadherin and the acquisition of N-cadherin are a hallmark of EMT (5). This mechanotransmission between N-cadherin and radioresistance has been shown in glioblastoma, as upregulation of N-cadherin triggers adaptive radioresistance through interaction with cadherin junctions and β-catenin [26, 27]. In breast cancer, the E-cadherin/N-cadherin switch is controlled by principal signalling pathways such as TGF-β, Wnt/β-catenin and Notch which is also the case with the data presented here, as TGF-β is reported to be activated after irradiation [5].

An important caveat with the functional invasion efficiency data Figure 2 is that the cadherin switch ratio alone cannot be used to predict the invasiveness. The switch ratio was the highest (1.80) at 2 Gy direct irradiation, while the invasion efficiency was the lowest (57.6%). This dissociation highlights the fact that cadherin switching is essential but not enough for functional invasion; other cofactors, such as the activity of MMPs, cytoskeletal remodeling and metabolic adaptation should be involved in making adhesion molecule switching into functional invasion output. The efficiency index of 129.7 for exposure to 2 Gy using exosome (with a similar cadherin switch ratio) implies that the exosomal pathway could serve as a source of such cofactors.

4.6. 3D Response Surface Mapping and Clinical Implications

The 3D topology figure shows the combinatorial effect of irradiation dose and time on invasion, which shows a steep synergistic slope at high dose (2 Gy) and late (long) timepoint with invasion >11,300 cells/field.This topology captures the central finding of the study: direct radiation produces a low-dose hyper-sensitive peak that subsequently plateaus, while exosome-mediated signalling produces a delayed, dose-dependent surge that exceeds direct effects by a wide margin at clinically relevant doses and extended timepoints Figure 7.

The clinical implications are twofold. Firstly, the delayed exosomal stream suggests that post-radiotherapy observation for metastatic potential should extend beyond the immediate treatment period, as the pro-invasive programming of bystander cells may appeared following exposure by days to weeks. Secondly, the exosomal signalling were identify as the dominant driver of sustained pro-invasive potentiation at 2 Gy provides a rationale for targeting exosome biogenesis or uptake as an adjunct to radiotherapy. These suggestion was supported by preclinical evidence includes the observation that co-treatment with vactosertib, a TGF-β receptor inhibitor, suppresses radiotherapy-induced EMT, stemness, and lung metastasis [2], in addition, the exosomal miR-21 from irradiated cells contributes to poorer prognosis in radiotherapy-treated patients [28]. The present data support the concept that the exosomal compartment represents a tractable therapeutic

target for mitigating the unintended pro-metastatic consequences of breast cancer radiotherapy, particularly at the 2 Gy fraction sizes in standard clinical use.

Limitations and Future Directions

This data comes from one cell line (MCF-7), which is estrogen receptor (ER) positive and lumenal in subtype; others like triple-negative (MDA-MB-231) could have a different baseline EMT plasticity and exosomal cargo. The Matrigel invasion assay is not a comprehensive metastasis model due to the presence of multiple factors not representative of in vivo metastasis such as immune interactions, endothelial barriers and organ-specific colonization. It will also be important to determine if pharmacologic inhibition of exosome release or specific cargo components can block the late-timepoint invasive surge, without affecting the tumoricidal activity of radiotherapy.

5. Conclusion

In conclusion, ionising radiation induces MCF-7 breast cancer cell invasion via two mechanisms that have opposing dynamics. Exosome-mediated bystander signalling resulted in a progressive, dose-dependent increase, peaking at 11,385 cells/field at 2 Gy (late time point) or by 2.38-fold compared to direct irradiation, whereas the direct irradiation response was non-linear with peak invasion at 0.1 Gy ($\sim$1.74-fold) which plateaued at 2 Gy. The Functional Invasion Efficiency Index showed that a direct exposure to radiation induces cadherin switching (1.80 at 2 Gy) but without functional invasion; however, the transformation induced by exosomal exposure is a coordinated up-regulation of N-cadherin and downstream invasion machinery (129.7 at 2 Gy). The results here highlight that the pro-metastatic potentiation occurs in a delayed manner and persists for a long time after exposure at clinically relevant dose levels, suggesting that targeting exosomes could be used as an adjunct to radiotherapy, and that even low doses could acutely promote EMT.

Article Information

Ethical Approval: Not applicable.

Informed Consent: Not applicable.

Consent for Publication: Not applicable.

Data Availability: The datasets generated and/or analyzed during the current study are available from the corresponding author upon reasonable request.

Clinical Trial Registration: Not applicable.

Funding: No external funding was received for this study.

Conflict of Interest: The authors declare that they have no conflict of interest.

Author Contributions: R.A.Z.A. - Conceptualization, Methodology, Investigation, Data Curation, Formal Analysis, Resources, Writing – Original Draft; K.I.T. - Formal Analysis, Resources, Writing – Original Draft; A.H.M. - Methodology, Investigation, Data Curation, Writing – Review & editing; S.A.B. - Conceptualization, Supervision; M.K. - Conceptualization, Supervision, Project Administration.

Acknowledgements: Grateful thanks to Mark Hill and James Thompson (MRC Oxford Institute for Radiation Oncology, University of Oxford) for assistance with the irradiations.
AI Use Disclosure: No generative artificial intelligence tools were used in the preparation of this manuscript.

References

[1] A. A. M. Alameen, H. M. Al-Kuraishy, A. I. Al-Gareeb, M. M. Shokr, and G. E. Batiha. Targeting of the PI3K/AKT/mTOR signaling pathway in the neurovascular interface in both Alzheimer's disease and atherosclerosis: The potential nexus. *Microvasc Res*, 166: 104947, 2026. URL https://doi.org/10.1016/j.mvr.2026.104947.

[2] J. Choi, J. Park, I. Cho, and Y. Sheen. Co-treatment with vactosertib, a novel, orally bioavailable activin receptor-like kinase 5 inhibitor, suppresses radiotherapy-induced epithelial-to-mesenchymal transition, cancer cell stemness, and lung metastasis of breast cancer. *Radiol Oncol*, 56(2):185–197, 2022. URL https://doi.org/10.2478/raon-2022-0012.

[3] X. Deng, C. Chen, F. Wu, L. Qiu, Q. Ke, R. Sun, Q. Duan, M. Luo, and Z. Luo. Curcumin Inhibits the Migration and Invasion of Non-Small-Cell Lung Cancer Cells Through Radiation-Induced Suppression of Epithelial-Mesenchymal Transition and Soluble E-Cadherin Expression. *Technol Cancer Res Treat*, 19:1533033820947485, 2020. URL https://doi.org/10.1177/1533033820947485.

[4] R. Al-Abedi, S. T. Cagatay, A. Mayah, S. A. Brooks, and M. Kadhim. Therapeutic Fractional Doses of Ionizing Radiation Promote Epithelial-Mesenchymal Transition, Enhanced Invasiveness, and Altered Glycosylation in MCF-7 Breast Cancer Cells. *Genome Integr*, 14:e20230001, 2023. URL https://doi.org/10.14293/genint.14.1.002.

[5] R. Al-Abedi, S. Tuncay Cagatay, A. Mayah, S. A. Brooks, and M. Kadhim. Ionising Radiation Promotes Invasive Potential of Breast Cancer Cells: The Role of Exosomes in the Process. *Int J Mol Sci*, 22(21):11570, 2021. URL https://doi.org/10.3390/ijms222111570.

[6] C. Han, C. Zhang, H. Wang, and L. Zhao. Exosome-mediated communication between tumor cells and tumor-associated macrophages: implications for tumor microenvironment. *Oncoimmunology*, 10(1):1887552, 2021. URL https://doi.org/10.1080/2162402x.2021.1887552.

[7] K. Kim, K. O. Jung, S. Oh, Y. H. Kim, S. Y. Lee, S. Hong, S. H. Cho, H. Kim, S. Rhee, G. J. Cheon, K. W. Kang, J. K. Chung, and H. Youn. Radiation-induced exosomal miR-21 enhances tumor proliferation and invasiveness in breast cancer: implications for poor prognosis in radiotherapy patients. *Exp Hematol Oncol*, 13(1):120, 2024. URL https://doi.org/10.1186/s40164-024-00585-5.

[8] M. S. Lach, J. P. Wróblewska, M. Michalak, B. Budny, E. Wrotkowska, and W. M. Suchorska. The Effect of Ionising Radiation on the Properties of Tumour-Derived Exosomes and Their Ability to Modify the Biology of Non-Irradiated Breast Cancer Cells-An In Vitro Study. *Int J Mol Sci*, 26(1):376, 2025. URL https://doi.org/10.3390/ijms26010376.

[9] B. Marples, P. Lambin, K. A. Skov, and M. C. Joiner. Low dose hyper-radiosensitivity and increased radioresistance in mammalian cells. *Int J Radiat Biol*, 71(6):721–735, 1997. URL https://doi.org/10.1080/095530097143725.

[10] L. A. Ryan, C. B. Seymour, M. C. Joiner, and C. E. Mothersill. Radiation-induced adaptive response is not seen in cell lines showing a bystander effect but is seen in lines showing HRS/IRR response. *Int J Radiat Biol*, 85(1):87–95, 2009. URL https://doi.org/10.1080/09553000802635062.

[11] H. Imaizumi, K. Minami, M. Hieda, N. Narihiro, and M. Koizumi. The linker of nucleoskeleton and cytoskeleton complex is required for X-ray-induced epithelial-mesenchymal transition. *J Radiat Res*, 64(2):358–368, 2023. URL https://doi.org/10.1093/jrr/rrac104.

[12] R. K. Kim, N. Kaushik, Y. Suh, K. C. Yoo, Y. H. Cui, M. J. Kim, H. J. Lee, I. G. Kim, and S. J. Lee. Radiation driven epithelial-mesenchymal transition is mediated by Notch signaling in breast cancer. *Oncotarget*, 7(33):53430–53442, 2016. URL https://doi.org/10.18632/oncotarget.10802.

[13] C. Martins-Lima, V. Miranda-Gonçalves, J. Lobo, V. Constâncio, P. Leite-Silva, C. Guimarães-Teixeira, S. Monteiro-Reis, J. P. Sequeira, M. Cantante, C. S. Gonçalves, B. M. Costa, R. Henrique, and C. Jerónimo. Cadherin switches during epithelial-mesenchymal transition: CDH_4/RCAD downregulation reduces bladder cancer progression. *Cell Oncol (Dordr)*, 45(1):135–149, 2022. URL https://doi.org/10.1007/s13402-021-00657-2.

[14] M. Ashrafizadeh, J. Dai, P. Torabian, N. Nabavi, A. R. Aref, A. A. A. Aljabali, M. Tambuwala, and M. Zhu. Circular RNAs in EMT-driven metastasis regulation: modulation of cancer cell plasticity, tumorigenesis and therapy resistance. *Cell Mol Life Sci*, 81(1):214, 2024. URL https://doi.org/10.1007/s00018-024-05236-w.

[15] G. Feng, L. Zhang, W. Bao, J. Ni, Y. Wang, Y. Huang, J. Lyv, X. Cao, T. Chen, K. You, H. Khan, and X. Shen. Gentisic acid prevents colorectal cancer metastasis via blocking GPR81-mediated DEPDC5 degradation. *Phytomedicine*, 129:155615, 2024. URL https://doi.org/10.1016/j.phymed.2024.155615.

[16] Y. Gao, J. Xie, Z. Yang, M. Li, H. Yuan, and R. Li. Functional tumor-derived exosomes in NSCLC progression and clinical implications. *Front Pharmacol*, 16:1485661, 2025. URL https://doi.org/10.3389/fphar.2025.1485661.

[17] W. Luo, Q. Shi, M. Han, Z. Zhang, R. J. Reiter, M. Ashrafizadeh, N. Nabavi, G. Sethi, C. Nicot, and Y. Mao. TGF-β-driven EMT in cancer progression and drug resistance. *Cytokine Growth Factor Rev*, 85:11–25, 2025. URL https://doi.org/10.1016/j.cytogfr.2025.05.004.

[18] C. Y. Loh, J. Y. Chai, T. F. Tang, W. F. Wong, G. Sethi, M. K. Shanmugam, P. P. Chong, and C. Y. Looi. The E-Cadherin and N-Cadherin Switch in Epithelial-to-Mesenchymal Transition: Signaling, Therapeutic Implications, and Challenges. *Cells*, 8(10):1118, 2019. URL https://doi.org/10.3390/cells8101118.

[19] S. Osuka, D. Zhu, Z. Zhang, C. Li, C. T. Stackhouse, O. Sampetrean, J. J. Olson, G. Y. Gillespie, H. Saya, C. D. Willey, and E. G. Van Meir. N-cadherin upregulation mediates adaptive radioresistance in glioblastoma. *J Clin Invest*, 131(6):e136098, 2021. URL https://doi.org/10.1172/jci136098.

[20] Z. Zhang, Z. Yao, Z. Zhang, L. Cui, L. Zhang, G. Qiu, X. Song, and S. Song. Local radiotherapy for murine breast cancer increases risk of metastasis by promoting the recruitment of M-MDSCs in lung. *Cancer Cell Int*, 23(1):107, 2023. URL https://doi.org/10.1186/s12935-023-02934-6.

[21] K. Jezierska, A. Sekowska, W. Podraza, H. Gronwald, and M. Łukowiak. The effect of ionising radiation on the physical properties of 3D-printed polymer boluses. *Radiat Environ Biophys*, 60(2):377–381, 2021. URL https://doi.org/10.1007/s00411-021-00892-z.

[22] X. Zhang, X. Li, N. Zhang, Q. Yang, and M. S. Moran. Low doses ionizing radiation enhances the invasiveness of breast cancer cells by inducing epithelial-mesenchymal transition. *Biochem Biophys Res Commun*, 412(1):188–192, 2011. URL https://doi.org/10.1016/j.bbrc.2011.07.074.

[23] L. D. Bertelsen, L. H. Nielsen, H. S. Christensen, M. Bøgsted, H. Gregersen, J. H. Bønløkke, and M. T. Severinsen. The risk of multiple myeloma associated with daily low-dose exposure to ionising radiation from radon decay. *Cancer Epidemiol*, 101:103024, 2026. URL https://doi.org/10.1016/j.canep.2026.103024.

[24] E. Cahide, A. Bayramov, M. Beler, D. Cansiz, I. Unal, G. Egilmezer, S. Yaltkaya, A. Karagoz, H. Gündüz, E. Emekli-Alturfan, and S. E. Yalcinkaya. Low dose ionising radiation elicits MPTP comparable alterations in locomotor Function, oxidative balance and mitochondrial homeostasis in zebrafish embryos. *Sci Rep*, 15(1):45322, 2025. URL https://doi.org/10.1038/s41598-025-29382-8.

[25] E. Elbakrawy, S. Kaur Bains, S. Bright, R. Al-Abedi, A. Mayah, E. Goodwin, and M. Kadhim. Radiation-Induced Senescence Bystander Effect: The Role of Exosomes. *Biology (Basel)*, 9(8):191, 2020. URL https://doi.org/10.3390/biology9080191.

[26] A. Ramezani, M. Rahnama, F. Mahmoudian, F. Shirazi, M. Ganji, S. Bakhshi, B. Khalesi, Z. S. Hashemi, and S. Khalili. Current Understanding of the Exosomes and Their Associated Biomolecules in the Glioblastoma Biology, Clinical Treatment, and Diagnosis. *J Neuroimmune Pharmacol*, 20(1):48, 2025. URL https://doi.org/10.1007/s11481-025-10204-7.

[27] Y. Afshar, N. Sharifi, A. Kamroo, N. Yazdanpanah, K. Saleki, and N. Rezaei. Implications of glioblastoma-derived exosomes in modifying the immune system: state-of-the-art and challenges. *Rev Neurosci*, 36(3):315–325, 2025. URL https://doi.org/10.1515/revneuro-2024-0095.

[28] Y. Su, Z. Huang, Y. Chen, J. Deng, Y. Huang, and W. Xiong. Exosomes from miR-21-5p-modified adipose-derived stem cells promote wound healing by regulating M2 macrophage polarization in a rodent model of pressure ulcer. *J Mol Histol*, 56(3):135, 2025. URL https://doi.org/10.1007/s10735-025-10407-5.